

## The Influence Analysis of Hamilton Chaos Phase Trajectory in Additive White Noise Channel

Fu Yongqing<sup>1</sup> and Li Xingyuan<sup>1</sup>

<sup>1</sup>College of Information and Communication Engineering, Harbin Engineering University, Harbin 150001, Heilongjiang, China  
[fuyongqing@hrbeu.edu.cn](mailto:fuyongqing@hrbeu.edu.cn), [lixingyuan@hrbeu.edu.cn](mailto:lixingyuan@hrbeu.edu.cn)

### Abstract

Previously a novel chaos  $M$ -ary modulation and demodulation method based on spatiotemporal chaos Hamilton oscillator was proposed and is applied in  $M$ -ary communication. Without chaos synchronization circumstance, the performance of communication has been improved in bandwidth efficiency, transmission efficiency and anti-white-noise performance compared with traditional communication method. Due to the working performance of zone partition demodulator is strictly connected with channel noise, it is necessary to study the influence of Hamilton phase trajectory deeply by the channel noise. In this paper, two methods for designing of the boundary of zone partition demodulator in additive white Gaussian noise are discussed, which are using statistics and curve fitting ways. Therefore, the problem about how to determine the boundary of zone partition demodulator in white noise is solved. Finally, the chaos  $M$ -ary communication system based on Hamilton oscillator is constructed and simulated in white noise channel. The result shows that the method proposed in this paper can improve the anti-white-noise performance of the whole communication system.

**Keywords:** Hamilton oscillator, white noise, zone partition demodulator, chaos  $M$ -ary communication

### 1. Introduction

In recent years Chaos theory has been developed very rapidly, and has been applied in many fields, such as [1-4]. Chaos is sensitive to initial value, unpredictable and disorderly, these characteristics makes chaotic systems unstable and aperiodic, making them naturally harder to identify and to predict. Recently, many researchers have been looking for ways to utilize the characteristics of chaos in communication systems, since Pecora *et al.*, [5] have realized the synchronization between two chaos systems in 1990, chaos communication has become research hotspot.

Although the research of chaos theory on communication application has developed rapidly, the research on  $M$ -ary communication scheme are not extensive and thorough enough. In the past four years, some  $M$ -ary chaotic spread spectrum communication schemes [6-8] have been proposed. To a certain degree, these schemes have reduced the requirements of the chaos synchronization, and have improved bit error rate performance of the chaotic spread spectrum system, but low bandwidth efficiency is their common shortcoming. Quadrature Differential Chaotic Phase Shift Keying Communication scheme [9] and Orthogonal Chaotic Vector Shift Keying scheme [10] are proposed respectively, these schemes have improved the information transmission rate under the reduced requirements of the chaos synchronization, that is, bandwidth efficiency has been improved to a certain extent, but the bit error rate has not been effectively improved. Literature [11] has proposed the method which separates dynamic chaotic system sequences to realize  $M$ -ary communication, it improves information transmission rate and bit error rate, but the cost is high system complexity.

In order to solve the above problems, a novel M-ary chaotic digital modulation and demodulation scheme based on Hamilton oscillator has been proposed in our previous research [12]. By using Hamilton map's high sensitivity to initial value and region controllable characteristics of phase trajectory, mapping relationship between digital information and Hamilton map phase trajectory regions is established. Then the digital information is embedded in the phase trajectory regions to complete baseband M-ary digital modulation. Thus the mapping from digital M-ary information to Hamilton oscillator's phase trajectory region is realized. Meanwhile, a digital information demodulation method by judging the phase trajectory region of received signal is proposed, namely zone partition demodulation (ZPD) method. However, as the working performance of chaos M-ary communication demodulator is so closely connected with channel noise, therefore in order to obtain the optimal design of ZPD, the research on the influences to the roughness of Hamilton modulated signal by the channel noise should be studied deeply. Here the mathematical analysis of designing Hamilton ZPD in additive white noise channel is given. Finally, the whole chaos 4-ary communication system is constructed on the computer, the result shows that the proposed method about designing the boundary of ZPD is correct. Since the proposed ZPD method belongs to non-coherent demodulation technology, no chaos synchronization is needed and symbol error rate performance of the system is improved.

## 2. M-ary Modulation and Demodulation Method Based on Hamilton Oscillator

### 2.1. Hamilton Oscillator Modulation Method

As known from literature [13], the Hamilton oscillator module used for chaos M-ary communication can be expressed as follows

$$\begin{cases} x_{k+1} = x_k - p \sin(\pi y_k / 2) \\ y_{k+1} = p \sin(\pi x_{k+1} / 2) + y_k \end{cases} \quad (1)$$

where  $x_k$  and  $y_k$  denote the K-th point outputs of Hamilton oscillator,  $p$  is the control parameter. The part phase diagram of Hamilton oscillator is shown in Figure 1.

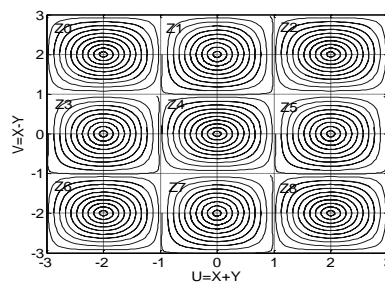


**Figure 1. The Part Phase Diagram of Hamilton Oscillator**

Figure 1 shows the phase diagram of Hamilton oscillator after coordinate transformation. Each ringlike trajectory is obtained by iterating equation (1) 50 times with initial values, and  $p$  is set to be 0.1. These phase trajectories are composed of nine cell flows which are regular arrangement, independent with each other, symmetrical in structure, and their locations and zone boundaries are relatively fixed without interference with each other as well. If we use  $Z_0, Z_1, Z_2, \dots, Z_8$  to denote the locations that every cell flow belongs to Figure 1, then the zone boundary can be expressed as  $u = 1 \pm 2a$ ,  $a = 0, 1, 2$ ;  $v = 1 \pm 2b$ ,  $b = 0, 1, 2$ ; and the area of each cell is  $2 \times 2$ .

According to the characteristics of Hamilton phase trajectories, here it is restricted that there is only one ring-like trajectory in each sub zone, then such zone can correspond with only one initial value, then one to one mapping relationship can be constructed between initial values and sub zones. Thus, when the initial value  $(x_{00}, y_{00})$  is substituted into equation (1) and iterated 50 times, a complete ring-like trajectory is obtained. By constructing the relationship between M-ary information and initial value of Hamilton oscillator, which can determine the sub zone, the M-ary information can be modulated by Hamilton oscillator.

It is noticed that Hamilton phase trajectory is a ring around its center, and it all falls into one square sub-region, thus Hamilton oscillator single ring phase trajectory can be approximated as circle line in order to reduce the computing complexity.

$$\begin{cases} u(t) = J + A\cos(2\pi f_0 t) \\ v(t) = K + A\sin(2\pi f_0 t) \end{cases} \quad (2)$$

where  $J, K \in n$ ,  $n = [0, \pm 1, \pm 2, \dots]$  donates the circle phase trajectory center point's abscissa and ordinate respectively;  $A < 1$  is radius of circle phase trajectory which is less than 1;  $f_0$  denotes the symbol rate of M-ary digital information, in order to ensure a complete circle phase trajectory is generated in every digital symbol period. Now the baseband signal's bandwidth after Hamilton modulation is  $B_\omega = f_0$ .

## 2.2. The Demodulation Method Based on Hamilton Oscillator Modulated signal

As the M-ary digital information is placed into the phase diagram of Hamilton oscillator, the signal can be demodulated from the phase diagram by using image partition technology [14]. The device which used this method is called zone partition demodulator (ZPD). At this moment, the design of zone partition detector shall take it as primary consideration, which every ring phase trajectory of Hamilton oscillator can be separated from phase plane. It can be satisfied by the Hamilton oscillator cell flow boundaries on the phase plane, so zone partition detector is expressed by numerical equation as follow.

$$Y(t) = \begin{cases} 1, & J-1 < \bar{u} < J+1 \& K-1 < \bar{v} < K+1 \\ 0, & \text{else} \end{cases} \quad (3)$$

Where  $J$  and  $K$  denote the circle phase trajectory center point's abscissa and ordinate respectively,  $Y(t)$  denotes the output of zone partition demodulator,  $\bar{u}$  and  $\bar{v}$  are Hamilton oscillator signals waiting for demodulation. According to equation (3), the zone partition detector is designed as shown in Figure 2.

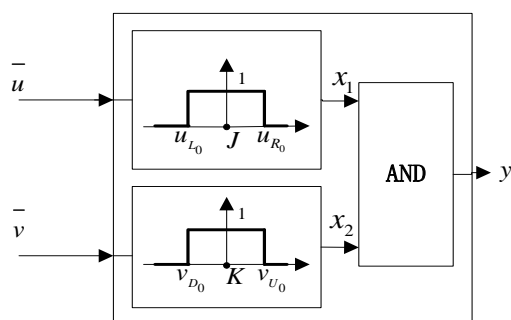
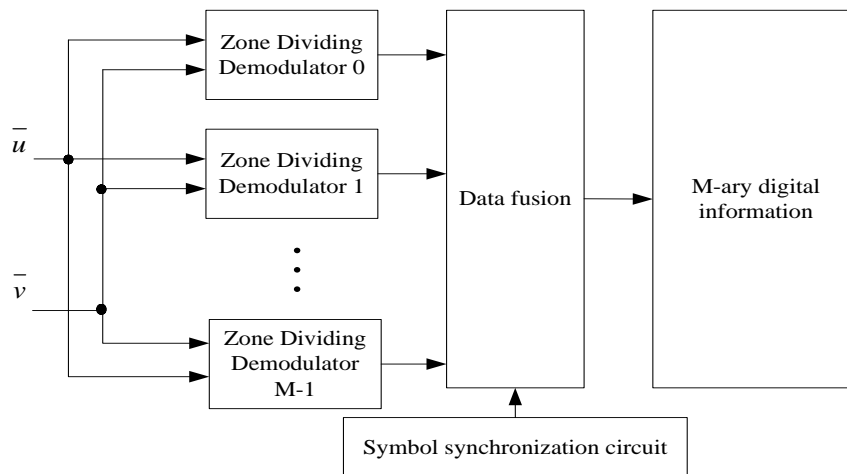


Figure 2. The Principle Structure of Zone Partition Demodulator

In Figure 2,  $u_{l_0} = J - 1$ ,  $u_{k_0} = J + 1$  are square region's left and right boundaries; respectively,  $v_{d_0} = K - 1$ ,  $v_{u_0} = K + 1$  are square region's down and up boundaries. The structure of M-ary zone partition demodulator is shown in Figure 3.



**Figure 3. The Structure of M-ary Demodulator**

### 3. The Construction Method of Chaos M-ary Demodulator in White Noise Channel

As shown in Figure 1, Hamilton modulated signals are distributed in the phase trajectories which is in two-dimensional plane, different signals are located into different phase zones, and do not interfere with each other. However, in chaos M-ary communication, when the modulated signals are transmitted to the receiver, the received signals will be disturbed by the channel noise, which can change the shape of the phase trajectory modulated by different digital information. The phase trajectory disturbed by the channel noise may pass through the sub zone, even interfere the other sub zones, which will reduce the demodulating performance of ZPD. In communication, SNR denotes the energy rate of signal to noise, average offset distance denotes offset effect of signal's phase trajectory in white noise channel. In order to get the optimal demodulating performance of ZPD, it is necessary to study the relationship between SNR and average offset distance of modulated signal's phase trajectory. Here, the boundary problem of demodulator in additive white gauss noise is solved by ways of statistics and curve fitting.

#### 3.1. The Curve Fitting Method to Determine the Boundary of ZPD

The curve fitting method is described as follows: Recording the samples of SNR and average offset distance through experiments, and draw it in two-dimensional axes, which SNR denotes X axes and average offset distance denotes Y axes, then reconstructing the formula relationship by curve fitting. Finally according to the formula, the boundary of ZPD can be determined. After a lot of experiments, it is shown that the Hamilton modulated signal's phase trajectory affected by the channel noise vibrates around the original phase trajectory. Here the chaos signals  $\bar{u}(t)$  and  $\bar{v}(t)$  after Radio-Frequency demodulation in the receiver are chosen for research. It is shown that the offset distance of  $\bar{u}(t)$  affected by the noise determines the left-right boundary of ZPD, and the offset distance of  $\bar{v}(t)$  affected by the noise determines the up-down boundary of ZPD. As shown in Figure 4:

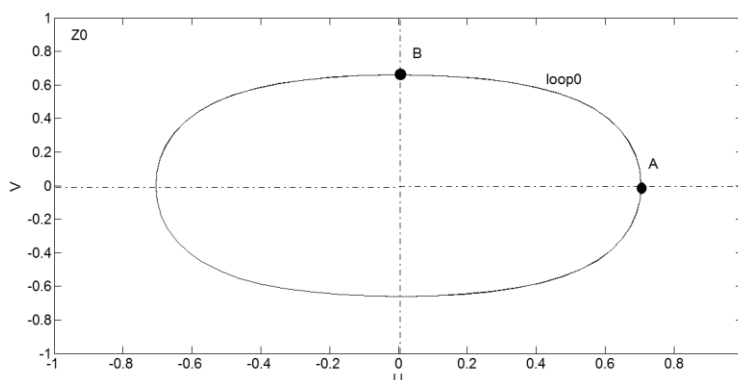


**Figure 4. The Phase Trajectory of One Hamilton Modulated Signals**

Here one circle phase trajectory of Hamilton modulated signal is chosen for study subject in the transmitter, “A” denotes the study point of  $\bar{u}(t)$ , which is cross point of phase trajectory with circle center in horizontal direction; “B” denotes the study point of  $\bar{v}(t)$ , which is cross point of phase trajectory with circle center in vertical direction. Due to “A” and “B” are the right-most and top-most point on the phase trajectory, these two points affected by the channel noise can lead to the largest zone of Hamilton phase trajectory, then it can be used for boundary design of ZPD. In the receiver, the modulated signals has been affected by the noise, therefore the “A” affected by the noise become “C” and “B” affected by the noise become “D” (it is assumed that “C” and “D” are all outside the phase trajectory). Then  $x$  denotes AC and  $y$  denotes BD, when SNR is given, the average offset distance PDD $_x$  and PDD $_y$  can be obtained respectively by averaging the samples of PDD $_x$  and PDD $_y$ .

Here chaos 4-ary communication is chosen, the modulated signals’ phase trajectory center coordinates are (8, 8), (8,-8), (-8,8), (-8,-8), the radius is 1V. After a large number of experiments, the relationship curve can be drawn between SNR and average offset distance. As shown in Figure 5 and Figure 6, the average offset distance is monotonously decreasing with the increasing of SNR.

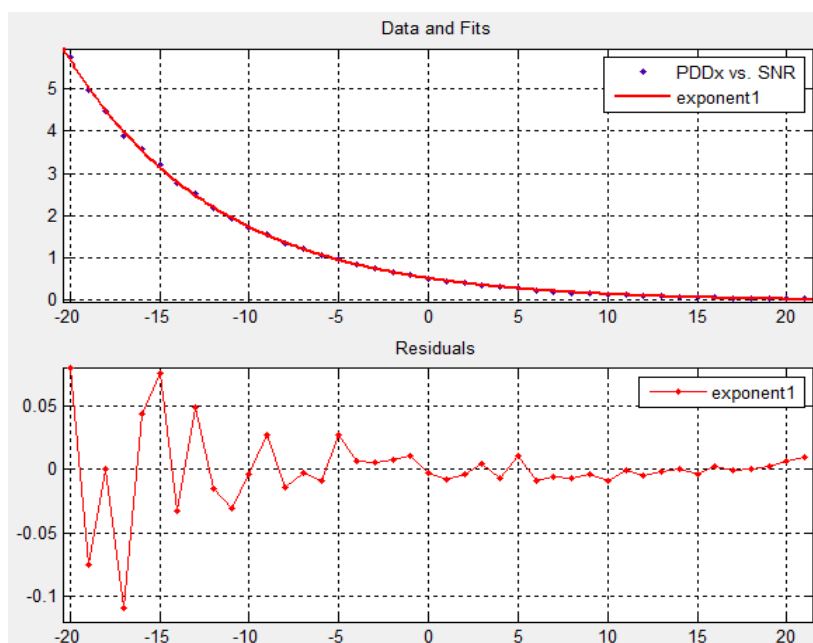


**Figure 5. The Curve Fitting and Residuals of  $u(t)$  in the Receiver with SNR**

The function after curve fitting is as follows:

$$f(x) = 0.5382e^{-0.1181x} - 0.02465e^{0.01002x} \quad (4)$$

The fitting statistical data is as follows: sum square error (SSE) is 0.03867; square of R (RS) is 0.9996; adjust square of R (ARS) is 0.9996; root mean square error (RMSE) is 0.0319. It is shown that the fitting effect is good. According to equation (4), the average offset distance can be obtained, then it is compared with the sample in Table 1. The relative error is controlled under 5 percent.

**Table 1. Chaos Signals  $u(t)$  after QAM Demodulation in AWGN**

| SNR                        | -20    | -16    | -12    | -8     | -4     | 0      | 4      | 8      | 12     | 16     |
|----------------------------|--------|--------|--------|--------|--------|--------|--------|--------|--------|--------|
| practical PDD <sub>x</sub> | 5.7658 | 3.5810 | 2.1822 | 1.3464 | 0.8460 | 0.5102 | 0.3024 | 0.1756 | 0.0979 | 0.0546 |
| estimate PDD <sub>x</sub>  | 5.6913 | 3.5401 | 2.1985 | 1.3617 | 0.8395 | 0.5136 | 0.3099 | 0.1825 | 0.1027 | 0.0524 |
| RE                         | 1.29%  | 1.14%  | 0.75%  | 1.14%  | 0.77%  | 0.67%  | 2.48%  | 3.93%  | 4.9%   | 4.03%  |

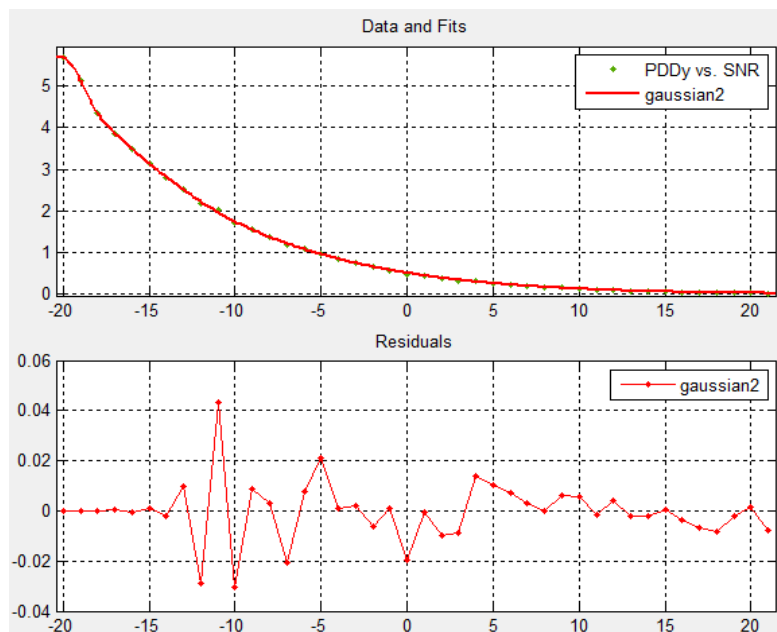


**Figure 6. The Curve Fitting and Residuals of  $v(t)$  in the Receiver with SNR**

The function after curve fitting is as follows:

$$f(y) = 0.7555 \exp\left[-\left(\frac{y+19.72}{1.308}\right)^2\right] + 0.2566 \exp\left[-\left(\frac{y+16.7}{4.437}\right)^2\right] - 0.03143 \exp\left[-\left(\frac{y+15.08}{1.072}\right)^2\right] + 50.81 \exp\left[-\left(\frac{y+70.23}{32.72}\right)^2\right] \quad (5)$$

The fitting statistical data: sum square error (SSE) is 0.006021; square of R (RS) is 0.9999; adjust square of R (ARS) is 0.9999; root mean square error (RMSE) is 0.01417. It is shown that the fitting effect is good. According to equation (5), the average offset distance can be obtained, then it is compared with the sample in Table 2. The relative error is controlled under 5 percent.

**Table 2. Chaos Signals  $v(t)$  after QAM Demodulation in AWGN**

| SNR                        | -20    | -16    | -12    | -8     | -4     | 0      | 4      | 8      | 12     | 16     |
|----------------------------|--------|--------|--------|--------|--------|--------|--------|--------|--------|--------|
| practical PDD <sub>y</sub> | 5.6846 | 3.4945 | 2.1959 | 1.3738 | 0.8460 | 0.4877 | 0.3096 | 0.1675 | 0.0960 | 0.0454 |
| estimate PDD <sub>y</sub>  | 5.6827 | 3.4935 | 2.2239 | 1.3701 | 0.8445 | 0.5072 | 0.2956 | 0.1672 | 0.0918 | 0.0489 |
| RS                         | 0.03%  | 0.03%  | 1.28%  | 0.27%  | 0.18%  | 3.99%  | 4.52%  | 0.18%  | 4.4%   | 7.71%  |

As seen in Table 1 and 2, when SNR is large than 0, the average offset distance of horizontal and vertical direction is both less than 0.6V.

In the receiver, after QAM demodulation, the amplitude of signals become half of the modulated signals in the transmitter, then the boundary of ZPD can be obtained according to equation 2.

$$\begin{cases} u_{L_0} \leq \frac{1}{2}(J - A) - PDDx \\ u_{R_0} \geq \frac{1}{2}(J + A) + PDDx \end{cases} \quad (6)$$

$$\begin{cases} v_{D_0} \leq \frac{1}{2}(K - A) - PDDy \\ v_{U_0} \geq \frac{1}{2}(K + A) + PDDy \end{cases} \quad (7)$$

The curve fitting method can construct the formula relationship of SNR and average offset distance without knowing the distribution of white noise in time domain, it can give the boundary of ZPD.

### 3.2. The Statistic Method to Determine the Boundary of ZPD

In this section, the relationship between band-limited additive white noise and phase trajectory of Hamilton modulated signal is discussed deeply. Without loss of generality, the channel is supposed to be Additive White Gaussian Noise (AWGN) channel, with zero mean value and its power spectrum density is  $N_0$ . Hamilton modulation is chosen in baseband, and QAM modulation is chosen in RF, as shown in Figure 7, the signal arriving at the receiver can be expressed as:

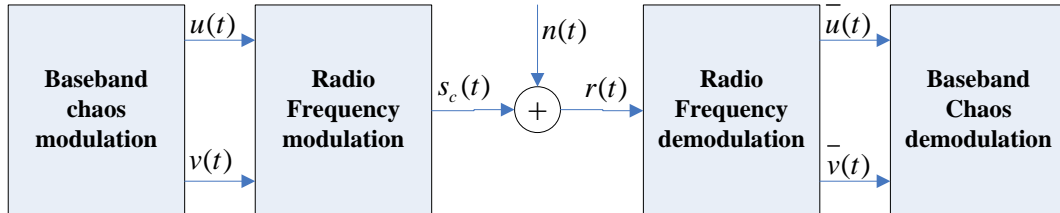


Figure 7. The Structure of Chaos M-ary Communication

$$r(t) = s_c(t) + n(t) \quad (8)$$

where  $s_c(t) = u(t)\cos(\omega_c t) + v(t)\sin(\omega_c t)$ ,  $\omega_c = 2\pi f_c$  is carrier angular frequency,  $u(t) = J + A\cos(2\pi f_0 t)$  and  $v(t) = K + A\sin(2\pi f_0 t)$  denote the Hamilton modulated signals.  $n(t)$  will become narrow band Gaussian random process after passing through band-pass filter and it can be expressed as:

$$\bar{n}(t) = a(t)\cos(\omega_c t) - b(t)\sin(\omega_c t) \quad (9)$$

where  $a(t)$  and  $b(t)$  are both stationary random process.

Therefore, after QAM demodulation and lowpass filtering, the baseband signal can be expressed as:

$$\begin{aligned}\bar{u}(t) &= LP\{(s_c(t) + \bar{n}(t)) \cos(\omega_c t)\} \\ &= \left[ (u(t) + a(t)) \cos(\omega_c t) + (v(t) - b(t)) \sin(\omega_c t) \right] \cos(\omega_c t) \Big|_{LPF} \\ &= \frac{1}{2} [u(t) + a(t)]\end{aligned}\quad (10)$$

where  $LP\{\square\}$  represents lowpass filtering, and its cut-off frequency is the maximum of baseband digital information frequency, which is much lower than carrier frequency  $\omega_c$ . In a similar way, we can get:

$$\bar{v}(t) = \frac{1}{2} [v(t) - b(t)] \quad (11)$$

Due to that the Hamilton modulated signal recovered by the receiver contains narrow band Gaussian noise, thus the roughness of reconstructed Hamilton phase trajectory will present to be statistic distribution under noise effect.

It is known that the correlation function of narrow band gauss noise appears to be sinc function in time domain, if the correct sample rate is chosen, then the statistical independence between the obtained sample values will be gotten. When the proper time  $t$  is given, sampling  $\bar{u}(t)$  and  $\bar{v}(t)$  we can get:

$$\begin{cases} \bar{u}_t = \frac{1}{2} (u_t + a_t) \\ \bar{v}_t = \frac{1}{2} (v_t - b_t) \end{cases} \quad (12)$$

where  $u_t$  and  $v_t$  are deterministic variables,  $a_t$  and  $b_t$  are gaussian random variables with zero mean value and  $\sigma_1^2$  variance, thus  $\bar{u}_t$  and  $\bar{v}_t$  are also gaussian random variables, their mean value and variance are as follows:

$$\begin{cases} E[\bar{u}_t] = \frac{1}{2} E[(u_t + a_t)] = \frac{1}{2} E[u_t] = \frac{1}{2} [J + A \cos(2\pi f_0 t)] \\ E[\bar{v}_t] = \frac{1}{2} E[(v_t - b_t)] = \frac{1}{2} E[v_t] = \frac{1}{2} [K + A \sin(2\pi f_0 t)] \end{cases} \quad (13)$$

$$D[\bar{u}_t] = \frac{1}{4} E[(a_t)^2] = \frac{1}{4} E[(b_t)^2] = D[\bar{v}_t] = \frac{1}{4} \sigma_1^2 \quad (14)$$

Therefore the probability density functions of  $\bar{u}_t$  and  $\bar{v}_t$  can be respectively expressed as:

$$\begin{cases} f_{\bar{u}}(\bar{u}_t) = \frac{1}{\sqrt{2\pi \frac{1}{4} \sigma_1^2}} \exp\left\{-\frac{[\bar{u}_t - E(\bar{u}_t)]^2}{\frac{1}{2} \sigma_1^2}\right\} \\ f_{\bar{v}}(\bar{v}_t) = \frac{1}{\sqrt{2\pi \frac{1}{4} \sigma_1^2}} \exp\left\{-\frac{[\bar{v}_t - E(\bar{v}_t)]^2}{\frac{1}{2} \sigma_1^2}\right\} \end{cases} \quad (15)$$



Since the mean values of  $\bar{u}_t$  and  $\bar{v}_t$  indicate to be the abscissa and ordinate of Hamilton phase trajectory center respectively. Obviously, the position of the center suffers from the effect of channel fading and noise. Let  $u_t - E[u_t]$  and  $v_t - E[v_t]$  represent the abscissa and ordinate values of Hamilton phase trajectory center under disturbing by the noise, marking  $\Delta r_{\bar{u}} = u_t - E[u_t]$  and  $\Delta r_{\bar{v}} = v_t - E[v_t]$ . According to probability theory, and in order to demodulate the signal exactly, the degree of confidence is set as follows:

$$\left\{ \begin{array}{l} P\left\{ \frac{|\bar{u}_t - E[\bar{u}_t]|}{\frac{1}{2}\sigma_1} \leq \delta_1 \right\} = 0.995 \\ P\left\{ \frac{|\bar{v}_t - E[\bar{v}_t]|}{\frac{1}{2}\sigma_1} \leq \delta_2 \right\} = 0.995 \end{array} \right. \quad (16)$$

where equation (16) denotes confidence interval, it means the most possible event's probability that occurs in  $\bar{u}_t$  and  $\bar{v}_t$ . Since  $\bar{u}_t$  and  $\bar{v}_t$  obey gauss distribution with  $(\frac{1}{2}E[\bar{u}_t], \frac{1}{4}\sigma_1^2)$  and  $(\frac{1}{2}E[\bar{v}_t], \frac{1}{4}\sigma_1^2)$  respectively, then they obey standard normal distribution after normalization. Thus we can get  $\delta_1$  and  $\delta_2$  through looking up standard normal distribution table, where  $\delta_1 = \delta_2 = 2.81$ . Therefore we have

$$\left\{ \begin{array}{l} |\Delta r_{\bar{u}}| \leq \frac{1}{2}\delta_1\sigma_1 = 1.405\sigma_1 \\ |\Delta r_{\bar{v}}| \leq \frac{1}{2}\delta_2\sigma_1 = 1.405\sigma_1 \end{array} \right. \quad (17)$$

In another hand, the signal-to-noise ratio (SNR) of the whole communication system is expressed as follows:

$$SNR = \rho = \frac{E_{sav}}{N_0} = \frac{P_{sav}}{N_0 B_w} = \frac{P_{sav}}{\sigma_1^2} \quad (18)$$

where  $P_{sav} = \frac{1}{T} \int_0^T s_c^2(t) dt = \frac{1}{T} \int_0^T [u^2(t) + v^2(t)] \cos^2(\omega_c t - \theta_m) dt$ ,

$\theta_m = \arctan(v/u)$ ,  $B = \frac{1}{T} = R_m$ ,  $T$  is symbol period. Since the signals  $u(t)$  and  $v(t)$

are given, then  $P_{sav} = \frac{1}{2}(J^2 + K^2 + A^2)$ , thus

$$\left\{ \begin{array}{l} |\Delta r_{\bar{u}}| \leq |\Delta r_{\bar{u}}|_{\max} = \frac{1}{2}\delta_1 \sqrt{\frac{P_{sav}}{\rho}} = 1.405 \sqrt{\frac{J^2 + K^2 + A^2}{2\rho}} \\ |\Delta r_{\bar{v}}| \leq |\Delta r_{\bar{v}}|_{\max} = \frac{1}{2}\delta_2 \sqrt{\frac{P_{sav}}{\rho}} = 1.405 \sqrt{\frac{J^2 + K^2 + A^2}{2\rho}} \end{array} \right. \quad (19)$$

The expression gives the relationship between the maximum roughness of the recovered signals' phase trajectory and SNR. Obviously, as SNR increases,  $|\Delta r_{\bar{u}}|_{\max}$  and  $|\Delta r_{\bar{v}}|_{\max}$  will decrease, they have inverse ratio relations.

According to (2), (8) and (19), we can know that the value of  $\bar{u}_t$  and  $\bar{v}_t$  have to drop the following range:

$$\begin{cases} \frac{1}{2}(J-A)-|\Delta r_{\bar{u}}|_{\max} \leq \bar{u}(t) \leq \frac{1}{2}(J+A)+|\Delta r_{\bar{u}}|_{\max} \\ \frac{1}{2}(K-A)-|\Delta r_{\bar{v}}|_{\max} \leq \bar{v}(t) \leq \frac{1}{2}(K+A)+|\Delta r_{\bar{v}}|_{\max} \end{cases} \quad (20)$$

Thus to determine the left-right and up-down boundary range of zone partition demodulator, only  $|\Delta r_{\bar{u}}|_{\max}$  and  $|\Delta r_{\bar{v}}|_{\max}$  are needed. The boundary range of zone partition demodulator can be selected as follows:

$$\begin{cases} u_{L_0} \leq \frac{1}{2}(J-A)-|\Delta r_{\bar{u}}|_{\max} \\ u_{R_0} \geq \frac{1}{2}(J+A)+|\Delta r_{\bar{u}}|_{\max} \end{cases} \quad (21)$$

$$\begin{cases} v_{D_0} \leq \frac{1}{2}(K-A)-|\Delta r_{\bar{v}}|_{\max} \\ v_{U_0} \geq \frac{1}{2}(K+A)+|\Delta r_{\bar{v}}|_{\max} \end{cases} \quad (22)$$

## 4. Theory Analysis and Evaluation

### 4.1. The Performance Evaluation of Hamilton M-ary Chaotic Communication System in White Noise Channel

In order to evaluate the performance of ZPD in chaos M-ary communication system, the Hamilton 4-ary chaotic communication system is constructed by employing the dynamic system analysis tool SystemView [15], as shown in Figure 8.

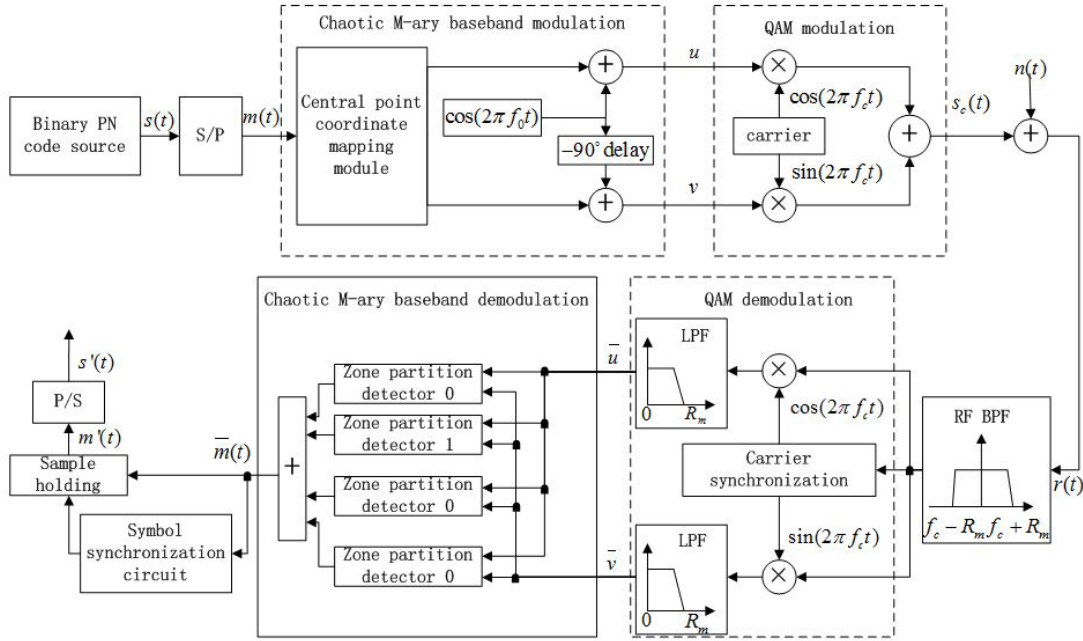


**Figure 8. The Structure of Hamilton Chaos 4-ary Communication System**

The parameters are set as follows:

(1) The data source  $s(t)$  is produced by a pseudo-random number (PN) sequence with rate 3.2Mbps.  $m(t)$  is 4-ary signal after serial parallel conversion, whose symbol rate  $R_m = 1.6\text{Mpsps}$ , *i.e.*, one-symbol-interval  $T = 0.65\mu\text{s}$ . Hamilton oscillator phase trajectory central point coordinates are  $(4, -4)$ ,  $(4, 4)$ ,  $(-4, 4)$ ,  $(-4, -4)$ , corresponding to digital symbol information 0, 1, 2, 3, respectively. The amplitude and frequency of quadrature sine wave which is generating Hamilton oscillator modulation signal is  $A = 0.5\text{V}$  and  $f_0 = 1.6\text{MHz}$ , respectively. The RF unit chooses QAM modulation, with frequency  $f_c = 50\text{MHz}$  and the amplitude is 1V.

(2) The channel chooses AWGN with power spectral density  $N_0$

(3) The central frequency and bandwidth of RF band-pass filter are  $f_c = 50\text{MHz}$  and 3.2MHz respectively. The cut-off frequency of low-pass filter is 1.6MHz.

(4) From section 3 it is known that the max roughness of Hamilton modulated signal  $|\Delta r_u|_{\max}$  and  $|\Delta r_v|_{\max}$  are all equal to 5.6419V, when SNR is 0. It is bigger than the distance between each two signals' center which is equal to 4. the phase trajectory of four signals will disturb with each other. However, when SNR increases, the roughness of signals' phase trajectory after QAM demodulation is decreasing. According to Equation (21), (22) the boundary of zone partition demodulator can choose designed as follows: when  $0 \leq \overline{u(t)} \leq 7.8919$  and  $-7.8919 \leq \overline{v(t)} \leq 0$ , then the ZPD outputs 0; when  $0 \leq \overline{u(t)} \leq 7.8919$  and  $0 \leq \overline{v(t)} \leq 7.8919$ , then the ZPD outputs 1; when  $-7.8919 \leq \overline{u(t)} \leq 0$  and  $0 \leq \overline{v(t)} \leq 7.8919$ , then the ZPD outputs 2; when  $-7.8919 \leq \overline{u(t)} \leq 0$  and  $-7.8919 \leq \overline{v(t)} \leq 0$ , then the ZPD outputs 3.

(5) The total system sample rate is  $f_s = 400\text{MHz}$ . In  $SNR = 10\text{dB}$ , relative simulated waveforms obtained by SystemView are shown in Figure 9:

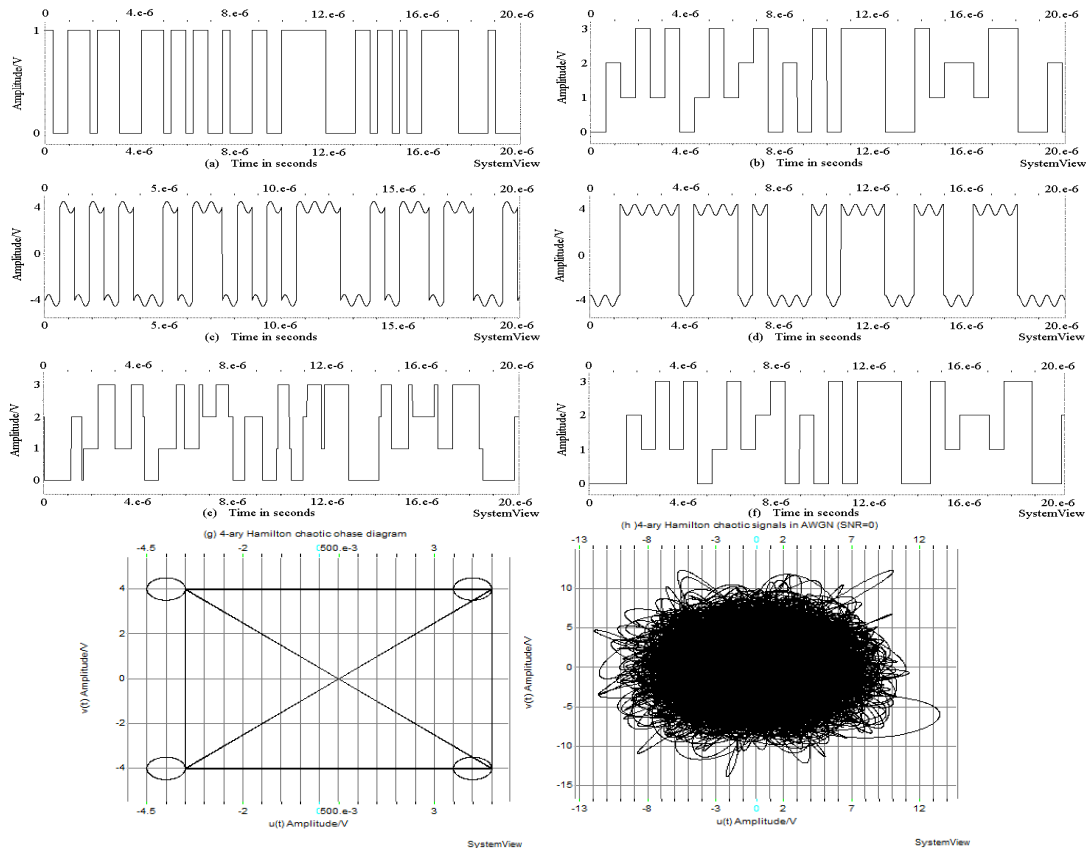


**Figure 9. (a) original binary information (b) 4-ary information after serial-parallel conversion (c)  $u(t)$  waveform after Hamilton chaotic modulation (d)  $v(t)$  waveform after Hamilton chaotic modulation (e) Signal waveform after zone partition demodulation in SNR=10 (f) Signal waveform after adjudicating by sampling**

As shown in Figure 9, the transmitted signals have been completely and exactly recovered by ZPD. In Figure 9 (g), each circle phase trajectory represents one symbol information, different zone where the circle embedded in represents different symbol information, and do not interfere with each other. However, in the receiver, the phase trajectory become disorder as shown in Figure 9 (h), the phase trajectory may pass through other zone, we can't use zone partition method with our eyes. In next section, the symbol error rate of Hamilton chaos 4-ary communication system in different boundary of ZPD is discussed.

#### 4.2. The Simulation Analysis of Symbol Error Characteristics of Hamilton M-ary Chaotic Communication System in Different Boundary of ZPD

In order to evaluate the symbol error rate performance of the proposed Hamilton M-ary chaotic communication system, the symbol average energy must be determined first. According to simulation parameter set up, the instant QAM carrier signal is expressed as follows:

$$s_c(t) = u(t) \cos \omega_c t + v(t) \sin \omega_c t = \sqrt{u^2(t) + v^2(t)} \cos(\omega_c t - \theta_m) \quad (23)$$

where  $\theta_m = \arctan(v/u)$ ,  $\omega_c = 2\pi f_c$ ,  $\omega_c = 2\pi f_c$ ,  $f_c = 50\text{MHz}$ ;  $u(t) = \pm 4 + 0.5 \cos \Omega t$ ,  $v(t) = \pm 4 + 0.5 \sin \Omega t$ , in which  $\Omega = 2\pi f_0$ ,  $f_0 = 1.6\text{MHz}$ .

Thus, QAM symbol average transmitting power is:

$$\begin{aligned}
 P_{sav} &= \frac{1}{T} \int_0^T s_c^2(t) dt = \frac{1}{T} \int_0^T [u^2(t) + v^2(t)] \cos^2(\omega_c t - \theta_m) dt \\
 &= \frac{1}{T} \int_0^T (16 \pm 4 \cos \Omega t + 0.25 \cos^2 \Omega t + 16 \pm 4 \sin \Omega t + 0.25 \sin^2 \Omega t) \cos^2(\omega_c t - \theta_m) dt \\
 &= \frac{1}{2T} \int_0^T (32.25 \pm 4 \cos \Omega t \pm 4 \sin \Omega t) dt \\
 &= 16.125W
 \end{aligned} \tag{24}$$

Therefore, in Hamilton oscillator M-ary chaotic QAM communication system, the ratio of symbol average energy to noisy power spectral density is expressed as

$$\frac{E_{sav}}{N_0} = \frac{P_{sav} T}{N_0} = \frac{P_{sav}}{N_0 B} \tag{25}$$

where  $B = \frac{1}{T} = R_m$  is equivalent baseband data bandwidth,  $T$  is symbol period,  $R_m = 1.6\text{MHz}$  is symbol rate.  $N_0$  is noisy power spectral density in the case of input impedance being one Ohm. According to (25), when  $E_{sav} / N_0$  is set with 0,1,...,15dB respectively, the corresponding channel noise power spectral density  $N_0$  is calculated and given in Table 3. In order to evaluate the demodulation performance of ZPD, three pairs of different boundary of ZPD is shown in Table 4. The symbol error rate of Hamilton 4-ary chaotic communication in white noise channel is drawn in Figure 10

**Table 3. The Simulation Parameters**

| $E_{sav} / N_0$ (dB) | $N_0$ (W/Hz) | $E_{sav} / N_0$ (dB) | $N_0$ (W/Hz) |
|----------------------|--------------|----------------------|--------------|
| 0                    | 10.0781e-6   | 8                    | 1.5973e-6    |
| 1                    | 8.0053e-6    | 9                    | 1.2688e-6    |
| 2                    | 6.3589e-6    | 10                   | 1.0078e-6    |
| 3                    | 5.0510e-6    | 11                   | 0.8005e-6    |
| 4                    | 4.0122e-6    | 12                   | 0.6359e-6    |
| 5                    | 3.4903e-6    | 13                   | 0.5051e-6    |
| 6                    | 2.5315e-6    | 14                   | 0.4012e-6    |
| 7                    | 2.0109e-6    | 15                   | 0.3490e-6    |

**Table 4. Different Boundary of ZPD in Different Scheme**

| Digital information<br>Scheme | 0  | 1  | 2  | 3  |
|-------------------------------|--|--|--|--|
| Scheme 1 (V)                  | $0 \leq \overline{u(t)} \leq 7.8919$<br>$-7.8919 \leq \overline{v(t)} \leq 0$      | $0 \leq \overline{u(t)} \leq 7.8919$<br>$0 \leq \overline{v(t)} \leq 7.8919$     | $-7.8919 \leq \overline{u(t)} \leq 0$<br>$0 \leq \overline{v(t)} \leq 7.8919$      | $-7.8919 \leq \overline{u(t)} \leq 0$<br>$-7.8919 \leq \overline{v(t)} \leq 0$       |
| Scheme 2 (V)                  | $0.5 \leq \overline{u(t)} \leq 7.3919$<br>$-7.3919 \leq \overline{v(t)} \leq -0.5$ | $0.5 \leq \overline{u(t)} \leq 7.3919$<br>$0.5 \leq \overline{v(t)} \leq 7.3919$ | $-7.3919 \leq \overline{u(t)} \leq -0.5$<br>$0.5 \leq \overline{v(t)} \leq 7.3919$ | $-7.3919 \leq \overline{u(t)} \leq -0.5$<br>$-7.3919 \leq \overline{v(t)} \leq -0.5$ |
| Scheme 3 (V)                  | $1 \leq \overline{u(t)} \leq 6.8919$<br>$-6.8919 \leq \overline{v(t)} \leq -1$     | $1 \leq \overline{u(t)} \leq 6.8919$<br>$1 \leq \overline{v(t)} \leq 6.8919$     | $-6.8919 \leq \overline{u(t)} \leq -1$<br>$1 \leq \overline{v(t)} \leq 6.8919$     | $-6.8919 \leq \overline{u(t)} \leq -1$<br>$-6.8919 \leq \overline{v(t)} \leq -1$     |

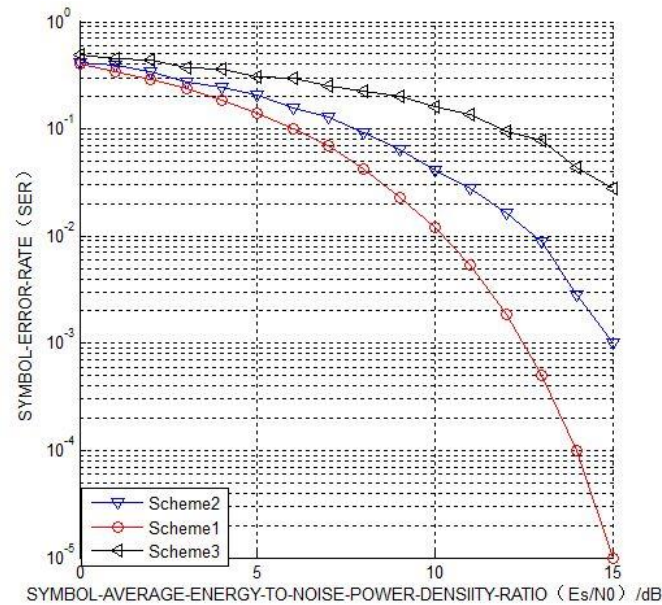


**Figure 10. SER curves of Hamilton Chaotic Communication System with Different boundary of ZPD in AWGN**

The Hamilton chaos 4-ary communication system chooses square-loop to recover carrier, and symbol synchronization selects non-linear filtering technology. The scheme 1 is the boundary derived from section 3; Scheme 2 is the boundary decreasing 0.5V based on scheme 1; Scheme 3 is the boundary decreasing 1V based on scheme 1. Due to scheme 1 chooses the critical boundary, if we increase the boundary based on scheme 1, the boundary will pass through the other zones' boundary, SER will increase. As seen in Figure 10, in white noise channel, the symbol error rates of Hamilton chaos 4-ary communication systems in three schemes are very different, the SER of scheme 1 improves about 2.5 dB than that of scheme 2, and improves about 6 dB than that of scheme 3. The result shows that the proposed method in this paper is correct, and different boundary of ZPD will influence the demodulation performance severely. Since M-ary chaotic modulation and demodulation method proposed in the paper needs to know phase trajectories of demodulating signal and phase trajectory region with information previously in order to demodulate information accurately, it is secure to non-corporation communications and has advantages of simple algorithm and easy to realize.

## 5. Conclusion

In this paper, the problem about designing the boundary of ZPD in Hamilton chaos M-ary communication system is studied in white noise channel. Two methods, which are of statistic and curve fitting, used for analysis about the roughness of chaos signals' phase trajectory in AWGN are given, and the formula form of ZPD's boundary is given, it has solved the designing problem of ZPD in AWGN. Finally, the Hamilton chaos 4-ary communication system in AWGN is constructed by employing SystemView, the validity and correctness of the proposed method are verified by the simulation. The superiority of the proposed system is that: the chaos signal is easy to generated, the system complexity is low, there is no need for chaos synchronization, the system has some security compared with traditional communication, and it has anti-noise performance improved.

## Acknowledgments

This work was supported by National Natural Science Foundations of China (Grant Nos. 61172038) and Central University Research Business Expenses Special Fund.

## References

- [1] W. H. Zhu, "Image encryption using CAT mapping and chaos approach", *International Journal of Signal Processing, Image Processing and Pattern Recognition*, vol. 7, no. 3, (2014), pp.331-340.
- [2] J. P. Bailey and A. N. Beal, "High-frequency reverse-time chaos generation using digital chaotic maps", *Electronics Letters*, vol. 50, no. 23, (2014), pp.1683-1685.
- [3] M. L. Barakat and A. S. Mansingka, "Hardware stream cipher with controllable chaos generator for colour image encryption", *IET Imag. Proc.*, vol. 8, no. 1, (2014), pp.33-43.
- [4] Q. Ye and L. L. Liang, "The Analysis and Application on a Fractional-Order Chaotic System", *TELKOMNIKA (Telecommunication Computing Electronics and Control)*, vol. 12, no. 1, (2014), pp. 23-32.
- [5] L. M. Pecora and T. L. Carroll, "Synchronization in chaotic systems", *Physical review letters*, vol. 64, no. 8, (1990), pp.821-824.
- [6] K. Y. Cheong, F. C. M. Lau and K. T. Chi, "Permutation-based M-ary chaotic-sequence spread-spectrum communication systems", *Circuits, Systems and Signal Processing*, vol. 22, no. 6, (2003), pp. 567-577.
- [7] H. Wang, J. Guo and Z. Wang, "Chaotic M-ary direct sequence spread spectrum signals blind dispreading", *Journal of Tsinghua University*, vol. 49, no. 1, (2009), pp.13-16.
- [8] M. Xu and H. Leung, "A Novel High Data Rate Modulation Scheme Based on Chaotic Signal Separation", *IEEE Transactions on communications*, vol. 58, no. 10, (2010), pp. 2855-2860.
- [9] S. Zhu, Y. Xu and K. Yin, "Design of a Quadrature Differential Chaotic Phase Shift Keying Communication System", *NSWCTC'09: International Conference on Networks Security, Wireless Communications and Trusted Computing*, Wuhan, China, (2009), pp. 518-521.
- [10] T. J. Wren and T. C. Yang, "Orthogonal chaotic vector shift keying in digital communications", *IET communications*, vol. 4, no. 6, (2010), pp.739-753.
- [11] S. Arai, Y. Nishio and T. Yamazato, "M-ary modulation scheme using separation of chaotic dynamics for noncoherent chaos-based communications", *Proc. NOLTA'09*, (2009), pp.312-315.
- [12] Y. Q. Fu and X. Y. Li, "Chaos M-ary modulation and demodulation method based on Hamilton oscillator and its application in communication", *Chaos: An Interdisciplinary Journal of Nonlinear Science*, 013111, vol. 23, no. 1, (2013).
- [13] F. S. Chen, "Chaos Control and Its Application", *China Electric Power Press*, Beijing (2004), pp.191-194.
- [14] Y. Q. Fu and D. M. Wu, "A circular zone partition method for identifying Duffing oscillator state transition and its application to BPSK signal demodulation", *Science China Information Sciences*, vol. 54, no. 6, (2011), pp.1274-1282.
- [15] *System View (Advanced Dynamic System Analysis) User Manual*, California USA: ELANIX Company, (1999), pp.1-291.

